Journal of Control, Automation and Electrical Systems (2022) 33:1601–1611
https://doi.org/10.1007/s40313-022-00907-0

Performance of Optimal Linear Filtering Methods for Signal Estimation in High-Energy Calorimetry

Guilherme Inácio Gonçalves[1] · Bernardo Sotto-Maior Peralva[2] · José Manoel de Seixas[3] · Luciano Manhães de Andrade Filho[4] · Augusto Santiago Cerqueira[4]

Received: 30 April 2021 / Revised: 19 December 2021 / Accepted: 29 January 2022 / Published online: 24 February 2022

Abstract
Discrete linear estimation methods, which are based on a weighted sum of the received time samples and the filter coefficients, are extensively employed in many applications. In conditions where the expected pulse shape is known and the received signal is mainly corrupted from additive Gaussian noise, such approaches perform close to the optimal operation. However, the readout signal may also suffer from pile-up, which potentially deteriorates the estimation process. In this paper, signal estimation is carried out for high-event rate experiments in high-energy physics, which aim at reconstructing particle collisions. In particular, the energies of the subproducts resulting from the collisions are measured by the calorimeter systems using shaped signals and estimating their amplitudes. The paper presents four linear estimation approaches and compares their performance in high signal pile-up conditions: two versions of an Optimal Filter that minimizes the noise variance impacts, a Wiener Filter to cope with the uncertainties arising from both the noise and the signal fluctuations, and a signal deconvolution technique that recovers the original signals within a calorimeter readout window. The efficiency is measured from simulated data where various signal pile-up scenarios and noise conditions are considered.

Keywords Signal estimation · Optimum filtering · Signal pile-up · Calorimeters · High-energy physics

1 Introduction

Signal estimation problems have been appeared in many fields such as communication (Yin and Cheng 2016), instrumentation (Collier and Zheng 2014) and experimental physics (Knoll 2010). A signal, usually corrupted from noise, must carry information that is usually related to one or a set of signal parameters such as amplitude, phase, frequency, length, etc.

Due to their simplicity and fast response, linear filters have extensively been employed for signal estimation tasks (Bos 2007; Kay 1993), especially in online applications (Vizireanu and Halunga 2012; Stoica et al. 2000; Pincibono and Duvalt 1988). However, under harsh conditions, where non-Gaussian components may arise embedded in the noise, the performance of linear methods may be deteriorated, introducing bias and increasing uncertainties in the measurement (Kay 1993). Often, nonlinear parameter estimation techniques become the proper solution (Bondon et al. 1992; Weng and Leung 2000).

In the field of high-energy physics, the experiments probe the properties of the elementary particles, as well as the

✉ Bernardo Sotto-Maior Peralva
bernardo.peralva@uerj.br

Guilherme Inácio Gonçalves
ginaciog@cern.ch

José Manoel de Seixas
seixas@lps.ufrj.br

Luciano Manhães de Andrade Filho
luciano.andrade@ufjf.br

Augusto Santiago Cerqueira
augusto.santiago@ufjf.br

1 Computational Modeling Graduate Program, Rio de Janeiro State University, Nova Friburgo, Brazil

2 Polytechnic Institute, Rio de Janeiro State University, Nova Friburgo, Brazil

3 Signal Processing Lab, COPPE/POLI, Federal University of Rio de Janeiro, Rio de Janeiro, Brazil

4 Electrical Engineering Graduate Program, Federal University of Juiz de Fora, Juiz de Fora, Brazil

fundamental interactions necessary to explain their behavior (Perkins 2000; Cottingham and Greenwood 1998). Frequently, particle accelerator facilities are built for performing particle collisions at very high-energy levels (up to TeV). Typically, two beams of particles traveling at approximately the speed of light are made to collide and the subproduct of these collisions are acquired and detected for reconstruction by high-precision experiments (Halpern 2010). Alternatively, fixed-target experiments (Halpern 2010) use a particle beam colliding with a target detector and producing secondary particles for specific studies. Several scientific discoveries were made possible through the use of particle accelerators including the existence of the Higgs boson in 2012 (The ATLAS and CMS Collaborations 2015), which was recognized through the Nobel prize of Physics in 2013.

In high-energy experiments, the calorimeter systems play a major role as they are responsible for absorbing and sampling the energy of the incoming particles, providing precise measurements of the energy flow (Wigmans 2017). They are also used for triggering on the physics of interest of the experiment and event selection tasks (Klein 1998). The information provided by the calorimeters is a key element to reconstruct the physics processes (Wigmans 2017). Typically, a calorimetry system is split into two sections, according to the type of particle interactions: electromagnetic and hadronic. They are usually segmented into layers, which produce up to hundreds of thousands of readout channels, which convert the original sensor information into electrical signals. The readout signals are then conditioned in such a way that pulse shapes are kept fixed along the dynamic range of the measurements and the signal amplitude becomes proportional to the signal energy (Anderson et al. 2005). Therefore, by simply estimating the signal amplitude, the energy can be extracted. The shaped signals from readout channels are typically digitized at the rate of the collision frequency.

The pile-up problem arises when the luminosity of the beam line increases significantly the channel occupancy level, which represents the probability of a collision to produce a particle that deposits an information (in terms of energy) in a given readout channel. As a result, more than one signal is acquired within a given readout window (Marshall and Atlas Collaboration 2014). This is the case of the Large Hadron Collider (LHC) experiments (Evans and Bryant 2008; Machikhiliyan 2009). The Out-Of-Time (OOT) signals distort the received signal and introduce challenges to the energy estimation methods (Marin 2020).

Currently, the Optimal Filter (Fullana 2006) algorithm is the most used method for estimating the amplitude from the incoming time samples in high-energy calorimetry. The OF approach is a simple and fast response linear filter that relies strongly on the calorimeter pulse shape information. The OF coefficients are computed through an optimization procedure that minimizes the noise variance impact on energy estimation subject to a set of constraints (Cleland and Stern 1994). It achieves optimal operation in conditions where the noise comprises only the typical (Gaussian) noise that comes from the electronics. However, since it does not take into account the pile-up in its design, the OF efficiency degrades under such conditions.

This paper presents different linear energy estimation algorithms currently available in modern calorimetry and provides performance comparisons considering various operation conditions. Apart from the OF method, a second method, called BLUE (Best Linear Unbiased Estimator) (Kay 1993), which is a variation from the OF algorithm, is also considered for performance comparison. Unlike the OF method, in the BLUE approach, the optimization procedure takes into account the signal pile-up effect and the number of constraints is smaller with respect to the OF strategy. The third method corresponds to the Wiener Filter (WF), and it aims at minimizing the square of the estimation error (Haykin 1998). Therefore, it tries to minimize all uncertainties from both the noise and the signal (due to phase deviations and deformities). It should be stressed that OF, BLUE and WF methods consider the signal pile-up as an additional noise component and use the second-order statistics to incorporate both the electronic readout noise and the signal pile-up components in the optimization procedure (Peralva 2015). The fourth method has been recently introduced as an alternative to the OF approach and is obtained through signal deconvolution and is called Multiple-Amplitude Estimator (MAE) (Andrade Filho et al. 2015). The MAE approach computes a linear transformation that recovers the amplitudes from the signals arising in a given readout window. As a result, unlike the OF and WF methods, the design of the MAE considers the electronic noise as the only source of noise, which can typically be modeled as a stationary white Gaussian process (The ATLAS Collaboration 2014; Gonçalves 2020).

The use of the linear methods for energy estimation has been evaluated and tested within the ATLAS Tile Calorimeter at LHC (Marin 2020). However, this paper extends the performance evaluation for a general-purpose calorimeter operating under severe conditions of signal phase deviations and channel occupancy levels. Particularly, the signal phase could be an issue under high event rate operation as performed by modern experiments where, for example, collisions are taking place every 25 ns like at the LHC (Evans and Bryant 2008). Apart from it, an energy estimation algorithm that can cope with signal phase deviations could also lead to simpler signal conditioning circuits.

The text is organized as follows. In the next section, the basic high-energy calorimetry principles are briefly introduced. In the Sect. 3, the energy estimators are described. The simulation results, considering different signal pile-up

conditions and pulse uncertainties, are shown in Sect. 4, and conclusions are derived in Sect. 5.

2 High-Energy Calorimeter System

Calorimeter readout signals are usually digitized for digital signal processing and may be unipolar or bipolar (Knoll 2010). The signal samples are sent to digital processors in which the signal amplitude is extracted. Here, without loss of generality, slightly asymmetric 150 ns width unipolar pulses are considered. The sampling frequency is 40 MHz, which is the bunch crossing rate for the LHC experiments, for instance (Evans and Bryant 2008).

Typically, the energy estimation is carried out by a linear combination of the received time samples (Adzic et al. 2006; Bertuccio et al. 1992). The noise covariance matrix is usually employed in the optimization process that computes the coefficients, in order to reduce the uncertainties in the measurements due to the electronic noise for each readout channel. However, the information from the signal pile-up introduces nonlinearities so that the noise distribution becomes non-Gaussian. Therefore, the efficiency of linear techniques is degraded and they become sub-optimal (Marin 2020). The effect of the signal pile-up is seen in Fig. 1, where the signal of interest is distorted by the presence of an OOT signal peaking at 50 ns, resulting in a deformed readout signal.

It should be stressed that the energy estimation efficiency strongly impacts on the selection of the calorimeter cells that are considered for the offline event reconstruction. For instance, particle showers emerging from the high-energy collisions and interacting with the calorimeter system may be reconstructed from topological clustering algorithms using the energy information from the individual readout channels.

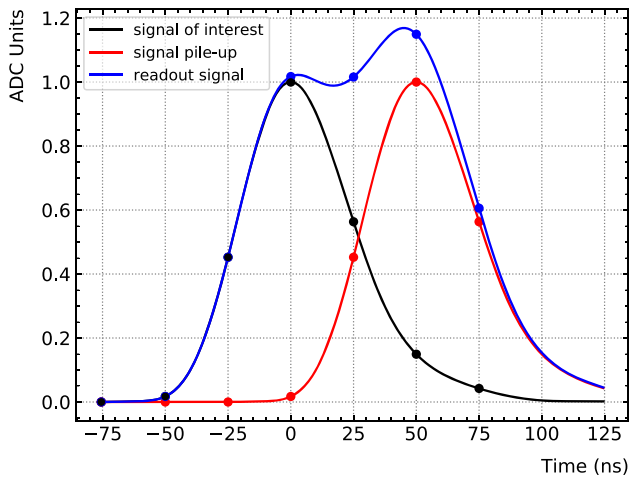

Fig. 1 Signal pile-up effect considering an unipolar readout pulse

This strategy aims at removing the calorimeter cells without significant information (Aad et al. 2017).

3 Linear Energy Estimation Methods

3.1 OF and BLUE Methods

Here, the BLUE approach is considered as a variation of the OF method. Therefore, the development is shown for the OF method and, whenever a difference from the methods needs to be emphasized, a comment is presented.

In both the OF and BLUE approaches, the received time samples $x[k]$, at instant k, are modeled as a first-order Taylor expansion:

$$x[k] = Ag[k] - A\tau\dot{g}[k] + n[k] + ped \tag{1}$$

where A is the pulse amplitude and $\mathbf{g}$ and $\dot{\mathbf{g}}$ are the vectors containing the reference normalized calorimeter pulse shape and its derivative, respectively. The vector $\mathbf{n}$ is the noise, τ is the phase deviation, and ped corresponds to the pulse offset typically added before the ADC conversion. The signal amplitude is estimated through a weighted sum given by:

$$\hat{A}_{OF} = \sum_{k=0}^{N-1} x[k]w[k] \tag{2}$$

where $w[k]$ are the OF weights and N corresponds to the number of time samples available.

In order to compute the filter weights $w[k]$ for an unbiased estimation, the expectation of the estimated amplitude $\hat{A}_{OF}$ must be equal to A. Therefore, considering a zero-mean noise ($\mathbb{E}\{n[k]\} = 0$), the following expression can be derived:

$$\mathbb{E}\{\hat{A}_{OF}\} = \sum_{k=0}^{N-1} (Aw[k]g[k] - A\tau w[k]\dot{g}[k] + w[k]ped) \tag{3}$$

In order to meet the unbiasing condition, three constraints are imposed:

$$\sum_{k=0}^{N-1} w[k]g[k] = 1 \tag{4}$$

$$\sum_{k=0}^{N-1} w[k]\dot{g}[k] = 0 \tag{5}$$

$$\sum_{k=0}^{N-1} w[k] = 0 \tag{6}$$

The first constraint guarantees the unbiasing main characteristics, while the second and third constraints make the estimator resilient against phase shifts and pedestal fluctuations. It should be mentioning that, for the BLUE method, the pedestal value is subtracted from the incoming signal time samples $x[k]$ before the filter operation. The pedestal value can be computed from calibration data taking and be stored in a database for use (Bella 2013). Therefore, the component $w[k]ped$ in Eq. (3) is suppressed as well as the constraint expressed in Eq. (6).

The variance for a linear estimator is minimized subject to the mentioned constraints. The variance is given by:

$$\mathbb{E}\{(\hat{A}_{OF} - A)^2\} = \sum_{k=0}^{N-1}\sum_{j=0}^{N-1} w[k]w[j]c[k,j] = \mathrm{w}^T\mathrm{Cw} \quad (7)$$

where $\mathbf{C}$ is the noise correlation matrix. Hence, the OF strategy depends on the actual information from the noise process, including the signal pile-up, which varies according to the operation conditions. To determine the set of weights $\mathbf{w}$, Eq. (7) must be minimized subject to the constraints defined in Eqs. (4), (5)–(6). The solution can be achieved by using Lagrange multipliers (Bertuccio et al. 1992) as

$$\mathrm{Bq}^T = \mathrm{z}^T \quad (8)$$

where

$$\mathbf{B} = \begin{pmatrix} c[1,1] & \cdots & c[1,N] & -g[1] & -\dot{g}[1] & -1 \\ \vdots & \ddots & \vdots & \vdots & \vdots & \vdots \\ c[N,1] & \cdots & c[N,N] & -g[N] & -\dot{g}[N] & -1 \\ g[1] & \cdots & g[N] & 0 & 0 & 0 \\ \dot{g}[1] & \cdots & \dot{g}[N] & 0 & 0 & 0 \\ 1 & \cdots & 1 & 0 & 0 & 0 \end{pmatrix} \quad (9)$$

$$\mathbf{q} = \begin{pmatrix} w[1] & w[2] & \ldots & w[N] & \lambda & \xi & v \end{pmatrix} \quad (10)$$

$$\mathbf{z} = \begin{pmatrix} 0 & 0 & \ldots & 0 & 1 & 0 & 0 \end{pmatrix} \quad (11)$$

The parameters λ, ξ and v correspond to the Lagrange multipliers. For the BLUE method, the last row and column from $\mathbf{B}$, as well as the last element from $\mathbf{z}$, are suppressed as the pedestal value is not an issue for it. Additionally, only the Lagrange multipliers λ and ξ are needed, and $\mathbf{v}$ is removed from $\mathbf{q}$. It is worth mentioning that, even in pile-up conditions, where the noise presents non-Gaussian properties, the noise correlation matrix $\mathbf{C}$ can still be used to minimize the noise Gaussian components. The OF and BLUE efficiencies increase considerably when using the correct noise correlation matrix (Peralva 2015).

3.2 Wiener Filtering

Unlike for the OF and MAE methods, where the pulse shape knowledge is required during the design phase, the WF approach does not need such information for its coefficient determination, as long as a simulated data set is provided. This algorithm was proposed envisaging energy estimation in very high channel occupancy conditions and uses the knowledge of the statistical properties of both the signal and the noise observations from a known data set. In this way, it reconstructs an optimal estimate of the signal from a noisy data stream. To this end, the weights are calculated using a simulation data set aiming at minimizing the expected value of the average squared of the error, given by:

$$J = \mathbb{E}\{e[.]^2\} \quad (12)$$

where the error $e[.]$ for a given signal is the difference between the estimated and reference amplitude $d[.]$ values as:

$$\mathbb{E}\{e[.]^2\} = \mathbb{E}\left\{\left(d[.] - \sum_{k=0}^{N-1} u[k]x[k]\right)^2\right\} \quad (13)$$

where the vector $x[k]$ corresponds to the received time samples and $u[k]$ corresponds to the filter weights. In order to minimize $\mathbf{J}$, it is necessary to compute its derivative as a function of $u[k]$ as follows:

$$\frac{\partial}{\partial u[k]} E\{e[.]^2\} = 0 \quad (14)$$

Setting Eq. (14) to zero produces the following expression:

$$\sum_{k=0}^{N-1} u[k]\mathbb{E}\{x[t-k]x[t-i]\} = \mathbb{E}\{x[t-k]d[t]\}, \quad (15)$$

where $i = 0, 1, \ldots, N-1$, and t is the time sample associated to a given readout window. From Eq. (15), it can be noted that:

1. $\mathbb{E}\{x[t-k]x[t-i]\}$ is the input autocorrelation matrix $\mathbf{R}$ for a given delay of $i-k$. This expression can be rewritten as:

$$r[i,k] = \frac{1}{N}\sum_{k=0}^{N-1} x[t-k]x[t-i]. \quad (16)$$

2. $\mathbb{E}\{x[t-k]d[t]\}$ corresponds to the cross-correlation between the input $x[t-k]$ and the reference output $d[t]$ (known from the simulation) for a given delay of $i-k$. It can also

be rewritten as

$$p[k] = \frac{1}{N}\sum_{t=0}^{N-1} x[t-k]d[t] \tag{17}$$

Equations (16) and (17) are known as Wiener–Hopf equations and are used in Eq. (15) producing the following expression:

$$\sum_{k=0}^{N-1} u[k]R[i,k] = p[k] \qquad k = 0, 1, \ldots, N-1\,. \tag{18}$$

Finally, the following equation can be used for computing the filter weights:

$$\mathbf{u} = \mathbf{R}^{-1}\mathbf{p} \tag{19}$$

In order to absorb bias (mean of the error), a fixed unitary element ("1") may be added to each input signal, as the last element. Thus, the amplitude estimated by the proposed algorithm is given by:

$$\hat{A}_{wiener} = \left(\sum_{k=0}^{N-1} u[k]x[k]\right) + u[N] \tag{20}$$

where $u[N]$ is the bias that is added to each estimate. It should be mentioned that, similarly as for the OF method, the computation of the WF coefficients depends on the second-order statistics. Thus, the coefficients should be recomputed for each operational condition in order to optimize the WF efficiency.

3.3 Multiple-Amplitude Estimator

The MAE method considers the out-of-time signals as additional pulses whose amplitudes are to be estimated (Andrade Filho et al. 2015). Considering a synchronized machine, such as the LHC, the MAE approach estimates a linear transformation based on the time shifted pulses, which are known from the reference pulse shape (output from the shaper circuit). As a result, the MAE design becomes independent from the OOT pile-up and it considers each channel energy deposition in a given collision as a Kronecker delta function (Oppenheim and Schafer 2009). Therefore, the received signal is considered as being the output of a linear and time invariant system (the calorimeter itself) fed from the original particle interaction.

If we consider a set of $a[k]$ energy depositions along the acquisition window, the received readout signal is expressed by:

$$y[k] = \sum_i (g[i]a[N-i]) + n[k] \tag{21}$$

The task is to estimate a linear transformation that recovers the amplitudes $a[k]$ from the received digitized pulse $y[k]$ as

$$\hat{\mathbf{a}}_z = \mathbf{W}_z^T\mathbf{y} \tag{22}$$

where

$$\mathbf{W}_z = \mathbf{C}_z^{-1}\mathbf{G}_z(\mathbf{G}_z^T\mathbf{C}_z^{-1}\mathbf{G}_z)^{-1} \tag{23}$$

The matrix $\mathbf{C}_z$ corresponds to the noise correlation matrix and $\mathbf{G}_z$ is composed by the shifted versions of the calorimeter reference pulse shape $g[k]$, where z is the number of signals present within a given calorimeter readout window. For example, in case $z = 7$, $\mathbf{G}_z$ is given by following matrix:

$$\mathbf{G}_z = \begin{bmatrix} g[4] & g[5] & g[6] & g[7] & 0 & 0 & 0 \\ g[3] & g[4] & g[5] & g[6] & g[7] & 0 & 0 \\ g[2] & g[3] & g[4] & g[5] & g[6] & g[7] & 0 \\ g[1] & g[2] & g[3] & g[4] & g[5] & g[6] & g[7] \\ 0 & g[1] & g[2] & g[3] & g[4] & g[5] & g[6] \\ 0 & 0 & g[1] & g[2] & g[3] & g[4] & g[5] \\ 0 & 0 & 0 & g[1] & g[2] & g[3] & g[4] \end{bmatrix} \tag{24}$$

and the amplitudes can be recovered from:

$$\hat{\mathbf{a}} = \mathbf{G}_z^{-1}\mathbf{y} \tag{25}$$

An interesting advantage of the MAE method is that the noise $n[k]$ remains modeled as zero-mean white Gaussian (electronic noise) and the noise correlation matrix is not needed for the design. It is worth mentioning that the pedestal value associated with a given readout channel is subtracted from the received time samples $x[k]$ before the MAE operation. Similarly as for the BLUE method, the pedestal value is typically recovered from a database where its value is computed using special calibration runs. Finally, a threshold is applied on the amplitude estimates in order to detect the presence of out-of-time signals so that the MAE executes its second step, using the same approach (Eq. (23)). This second step aims at reducing the estimator variance (resolution) by avoiding computing energies at empty positions within the readout window.

4 Results

The energy estimation methods were applied to simulated calorimeter signals considering different operation conditions. For efficiency evaluation, the performance of the

described methods was measured in terms of the estimation error and signal reconstruction quality.

4.1 Data Set

The simulation model refers to a single calorimeter readout channel response. For this, a 150 ns slightly asymmetric unipolar pulse, sampled at 40 MHz, was synthetized and seven time samples were used to represent the entire pulse. Unipolar pulse shaping has been chosen in different modern calorimeters (Anderson et al. 2005; Cadwell et al. 1992; Muller et al. 2006).

For the electronic noise model, a zero-mean Gaussian random variable with 20 MeV of standard deviation was used, as such a noise level may be considered typical in modern calorimetry (Adzic et al. 2006; Marjanovic 2019). Concerning the energy deposit within a readout channel, an exponential random variable with 300 MeV of mean value was chosen as it represents a typical calorimeter energy deposition from particle colliders (Wigmans 2017). Different signal pile-up conditions were tested, translated into different channel occupancy levels, reaching up to 90%. Additionally, in order to test the efficiency of the methods when the signal phase is an issue, time uncertainties were added to the readout signal. This parameter was modeled by a zero-mean Gaussian random variable with a standard deviation of 8 ns. A small pulse deformity was also introduced to the readout pulse on each digitized sample, modeled by a zero-mean Gaussian distribution, but with standard deviation of 1% with respect to the associated time sample index from the reference pulse shape.

The data set for each occupancy level comprised one million events that were equally divided into two subsets: development (used for designing the estimation methods) and test (used to evaluate their efficiency). Both the development and test sets comprise the usual electronic noise and the same signal pile-up conditions. However, for the test set, a signal whose amplitude is to be estimated by each method was added to each event. Similarly as for the signal pile-up, the amplitude was also modeled by an exponential random variable, but now with mean value equal to 900 MeV, in order to emulate nominal operation conditions for the trigger system (Aaij et al. 2019).

It is worth mentioning that all the simulation was carried out by a dedicated software tool, where the details concerning the data production and evaluation analysis can be found at (Gonçalves 2021).

4.2 Designing the Estimators

The filter designs extracted different information from the development data sets. For the OF and BLUE methods, the development sets provided the noise correlation matrices, while MAE assessed the pedestal estimation, which must be subtracted from the incoming time samples. Concerning the WF designs, their coefficients were designed from signals of interest immersed in electronic noise and signal pile-up, whose actual amplitude values were known a priori. It is worth mentioning that, for the development sets, it is important to assign the same probability of occurrence along the considered dynamic range. Thus, the signal amplitudes followed a uniform distribution in the range of [0; 10] GeV, in this case.

4.3 Performance Evaluations

The estimation errors (E_r) were computed by subtracting the estimated signal amplitudes (energy) $\hat{A}[i]$ from the true amplitude values $d[i]$ for each signal i as:

$$E_r[i] = \hat{A}[i] - d[i] \tag{26}$$

The mean and RMS error values were used to estimate both the bias and error bars achieved by each method. Additionally, the quality of the event reconstruction is also assessed. Here, the quality factor (QF) measures how well the input pulse (time samples) is reconstructed (Delmastro 2009) and it is defined as:

$$QF = \frac{1}{\hat{A}} \sqrt{\sum_{k=0}^{N-1} \frac{((r'[k] + ped) - x[k])^2}{N}} \tag{27}$$

where the elements $r'[k]$ and $x[k]$ represent the reconstructed and received samples for a given time sample k, respectively. The reconstructed pulse is computed using the amplitude values estimated by each method, and the reference calorimeter pulse shape $\mathbf{g}$. The $\hat{A}$ corresponds to the estimated amplitude performed by the method and ped parameter is the signal baseline. In practice, apart from selecting good reconstructed signals, the quality factor may also be used to flag corrupted data (Seixas 2015).

The impact of signal phase in energy estimation was evaluated considering not only a small phase deviation range (within ± 1 ns), which represents the conditions found in state-of-art calibrated calorimeters, such as the ones in LHC experiments (Fullana 2006; Adzic et al. 2006), but also for a general-purpose calorimeter with larger signal phase deviation values (up to approximately ± 20 ns).

4.3.1 Small signal phase deviation

Here, the signal phase is not a critical issue. Figure 2 shows the estimation error histograms for 30% of occupancy. It can be seen that the MAE method presents the sharper distribution, indicating the best performance. Evaluating only the

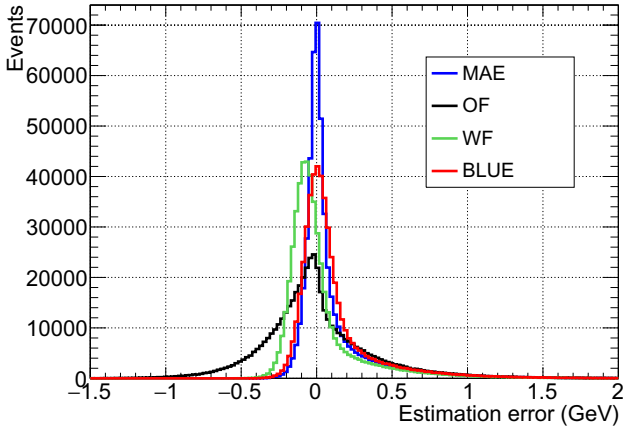

Fig. 2 Estimation error distributions considering a readout channel occupancy level of 30% and a small phase deviation

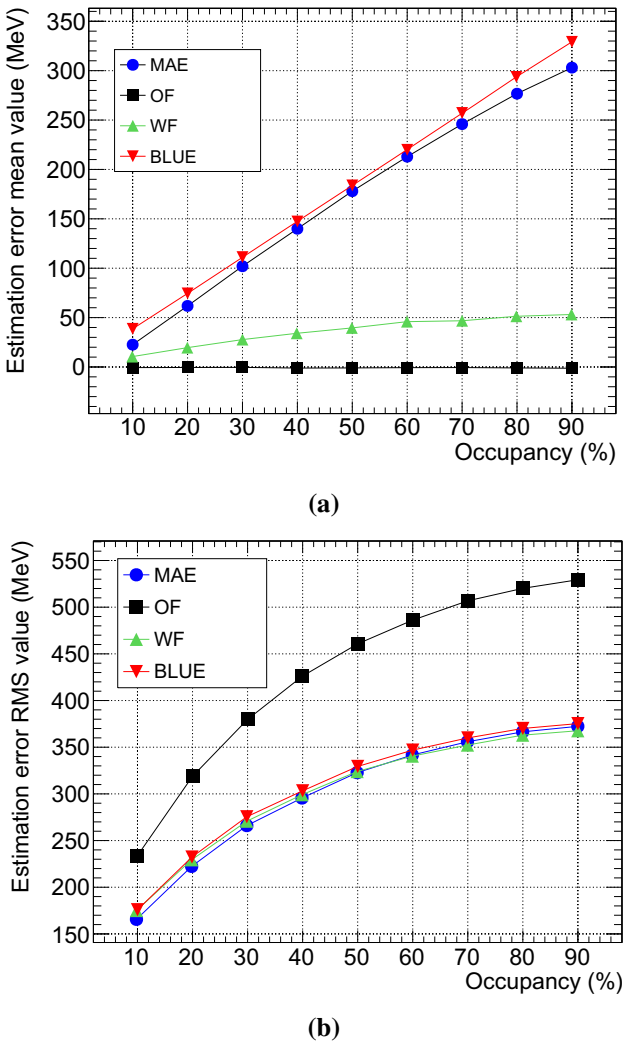

Fig. 3 Estimated mean **a** and RMS **b** error values as a function of the readout channel occupancy levels and considering a small signal phase deviation

mean and RMS, Fig. 3 shows the values achieved from each method considering a phase deviation range of ± 1 ns, considering different occupancy levels. As expected, under such conditions, the signal pile-up was the main source of uncertainties. In terms of the estimation error RMS value, the OF method presented the worst efficiency, while the other three methods showed similar performance, despite their linear increase in the mean estimation error. Unlike for the estimation error RMS, it should be stressed that the estimation error mean value may be corrected by a parametric function.

Since the estimation error distributions are not symmetrical, the RMS values may not properly reflect the methods' efficiency, although they provide valuable insights of their performance. Therefore, the QF values were computed in order to better assess the overall efficiency from the considered methods. Figure 4 shows the quality factor distributions for the 30% occupancy condition and the RMS values of the quality factor distributions as a function of the occupancy level. Under these conditions, it can be noted the best efficiency achieved by the MAE method with respect to the other methods. This can be explained by the MAE strategy to deal with the signal pile-up, where it estimates not only the amplitude of signal of interest as the other methods, but also from all possible OOT pulses present within a given readout window. Hence, the OOT signals are also taken into account to compute the quality factor, improving the received signal reconstruction efficiency.

4.3.2 Large Signal Phase Deviation

Next, the performance evaluation was extended to comprise large signal phase deviations (all values from the phase deviation model of a zero-mean Gaussian with 8 ns of standard deviation). The goal was to push the operation limits, including both high signal pile-up and large signal phase deviation conditions. Under these harsh signal phase conditions, Fig. 5 shows the achieved distributions for a 50% of readout channel occupancy. It can be noted that, for this condition, the WF method presented a sharper peak, indicating a better performance in terms of the estimator's variance. However, the WF distribution presented a larger positive tail and its distribution was slightly shifted towards the left, in order to preserve a close-to-zero mean value (as from the additional weight shown in Eq. (20)). The distributions for both MAE, BLUE and OF methods proved to be more symmetrical, with the peak of the distributions close to zero.

In order to evaluate the efficiency as a function of the occupancy level, Fig. 6 shows the mean and RMS values obtained from the estimation error distributions. It can be seen that the WF approach exhibited a better performance, as it presented the smallest RMS values along the occupancy range. Concerning the estimation mean error, both OF and WF could handle the pile-up better in such large signal phase

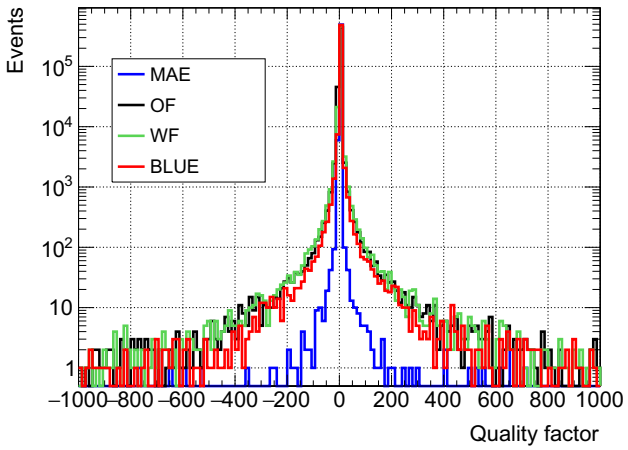

(a)

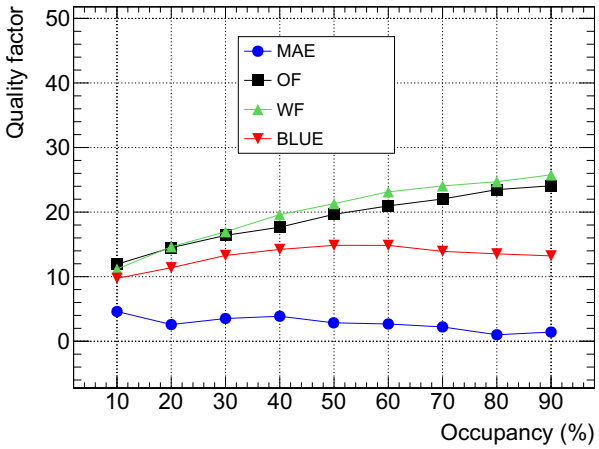

(b)

Fig. 4 Quality factor distributions for an occupancy of 30% **a** and **b** RMS values from the quality factor distributions as a function of the readout channel occupancy levels and considering a small signal phase deviation

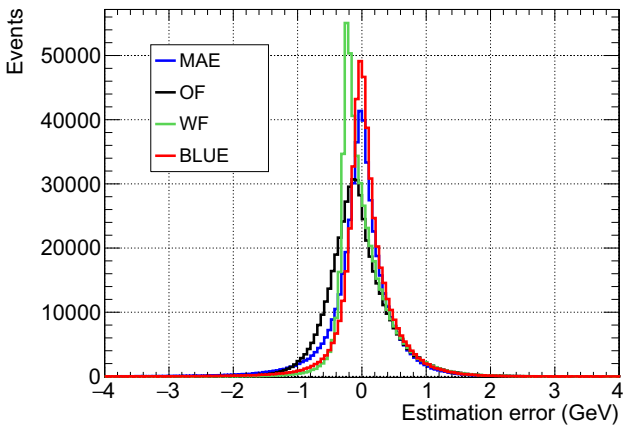

Fig. 5 Estimation error distributions considering a readout channel occupancy level of 50% and a large phase deviation

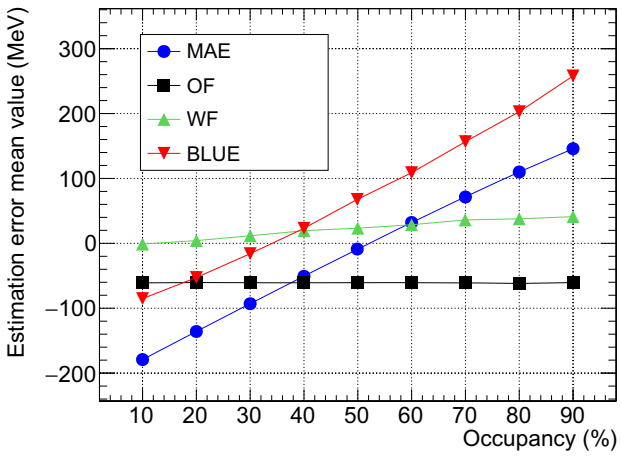

(a)

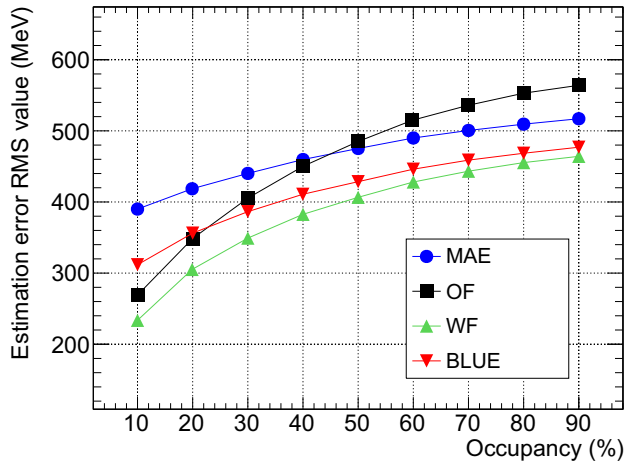

(b)

Fig. 6 Estimation error in terms of mean **a** and RMS **b** values as a function of the readout channel occupancy level and considering a large signal phase deviation

deviation conditions. While OF uses a constraint that forces the mean of the noise to be equal to zero [see Eq. (5)], the WF method considers the additional weight to compensate for the offset. The difference between these two strategies is that WF takes into account the uncertainties from both the noise and the signal, whereas the OF method considers only the noise component. Hence, as it can be depicted from Fig. 6a, the OF error mean value presented an almost fixed mean error value close to -60 MeV, as the signal phase was not taken into account in the design. In the other hand, the MAE and BLUE methods could not handle well such large signal phase deviation.

In order to become unbiased, a parametric equation may be computed to compensate for the mean error value resulting from each occupancy level. One can take advantage of the linear behavior expressed by the MAE estimation, for instance. This is qualitatively illustrated in Fig. 7a. Moreover, in order to evaluate the behavior of the fitting parameters as

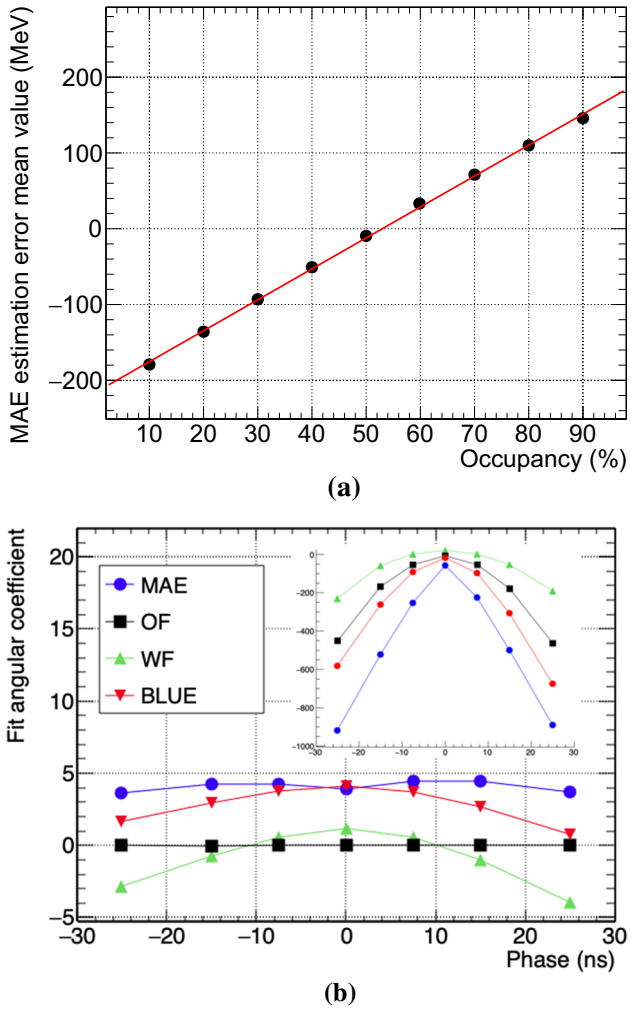

Fig. 7 Linear regression applied to the MAE's mean estimation error considering a large signal phase condition **(a)**, and the angular fitting parameters as a function of the signal phase, where the corresponding linear fitting parameters are embedded in the figure **(b)**

a function of the signal phase, Fig. 7b shows the angular fitting coefficients, whereas the corresponding linear parameters are shown in the plot embedded in the figure. Under these demanding occupancy and phase deviation conditions, the MAE method presents a larger angular and a more sensitive linear components with respect to the other methods, indicating that the linear correction is needed for this method to properly operate. As it was expected, the OF error mean value remains constant (angular coefficient close to zero), although its linear fitting component follows a second-order function, approximately, as it is the case for the BLUE and WF approaches.

Table 1 summarizes the linear fitting parameters for each method. All algorithms presented a good linear fitting quality, showing that the signal pile-up linearly introduces an energy bias that can be compensated for. It should be noticed that the OF method was capable of dealing with any noise offset

Table 1 Linear fitting parameters for the mean estimation error, considering a large phase deviation condition

Method	Linear coef. (MeV)	Ang. coef.
MAE	-217.90 ± 1.94	4.11 ± 0.04
OF	-60.80 ± 0.24	-0.01 ± 0.01
WF	-3.54 ± 1.26	0.52 ± 0.02
BLUE	-140.70 ± 6.27	4.28 ± 0.11

(see Eq. (6)) as its angular coefficient was almost zero. The linear coefficient of about -60 MeV was due to the signal uncertainties (mainly phase deviations), which such a design can not optimally cope with. Among the four methods, the MAE method showed to suffer more from the signal phase deviations as its linear fitting coefficient presented the larger absolute value (ideally, it should be close to zero). This can be explained by the fact that the MAE method relies on the information from several well-defined shifted pulse shapes, and it struggles to do so in conditions where the pulse shapes become deformed by phase deviations. Concerning the WF method, it exhibited the best resilience against the phase deviations, since it takes into account both the noise and the signal features in its optimization procedure.

While the mean estimation error could be parameterized for the introduced bias, the RMS of the estimation error could not be corrected for, as it is shown in Fig. 8 considering a 50% of occupancy. As from Fig. 8, the MAE and BLUE methods presented the best efficiencies for small signal phase values, which would be the case for the general-purpose LHC experiment (ATLAS and CMS) calorimeters, for instance. It should be noted that the coefficients from the OF, WF and BLUE methods need to be updated according to the occupancy level, while the MAE design does not need any information regarding the noise. In the other hand, if the phase absolute value increases, it becomes an issue for the MAE method, and the WF proved to perform better under such harsh conditions. Despite a reasonably good resilience against phase deviations, OF efficiency was surpassed by both MAE and BLUE methods for phase deviations within approximately ± 10 ns.

Similarly as performed for the small phase deviation conditions, the QF values from the signal reconstruction achieved by each method are computed. Figure 9 shows the distribution of the QF values considering the condition of 50% occupancy, and the RMS values from the quality factors as a function of the occupancy level. As it can be noticed, although the signal phase may be an issue for the MAE method, it still presents better signal reconstruction capabilities, with respect to the other considered methods.

5 Conclusions

This paper addressed the signal amplitude estimation problem for energy reconstruction based on high-energy calorime-

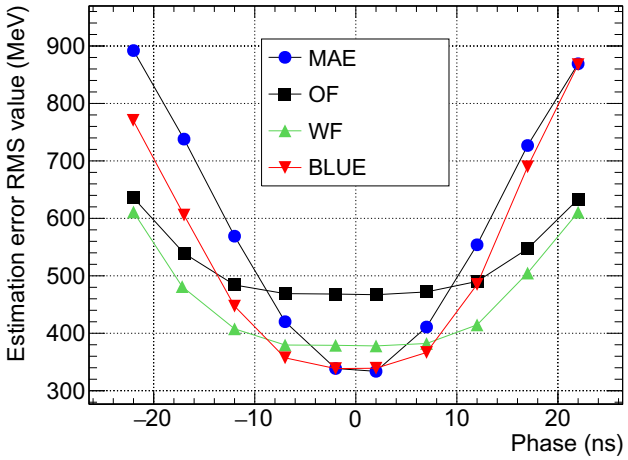

Fig. 8 The RMS estimation error evolution as a function of the signal phase deviation, considering a occupancy level of 50%

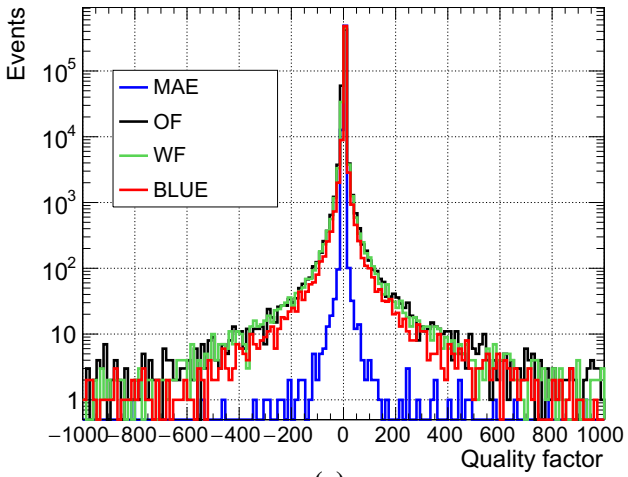

(a)

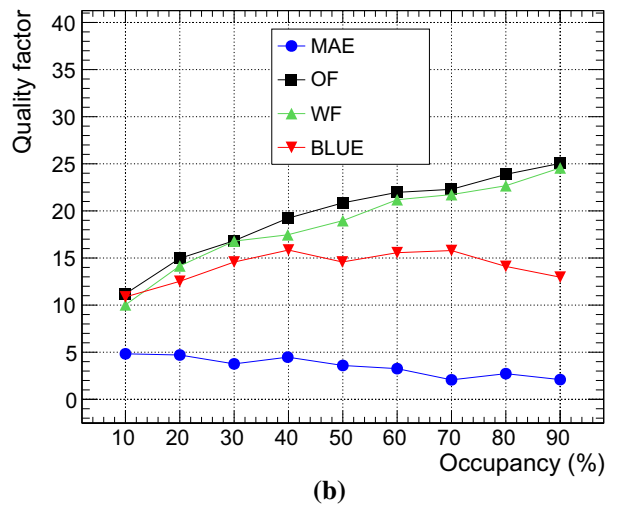

(b)

Fig. 9 Quality factor distributions for an occupancy of 50% **a** and **b** RMS values from the quality factor distributions as a function of the readout channel occupancy levels and considering a large signal phase deviation

ter systems, when they are submitted to severe signal pile-up conditions and pulse deformation from phase deviations becomes more significant. The achieved performance from different linear methods (OF, BLUE, WF and MAE) was compared in terms of the estimation error and signal reconstruction quality.

Using simulated signals, results showed that the MAE and WF methods achieved the best efficiency in terms of the estimation error RMS, when the signal phase is not an issue regardless the channel occupancy level. Additionally, under these conditions, the MAE presented a better capability of reconstructing the received signal, showing better quality factor values due to its strategy of deconvoluting the OOT signals. In the other hand, if on the top of the signal pile-up the signal phase becomes an issue, the WF was the best solution due to its capabilities to capture the signal uncertainties (phase and deformation) in its optimization procedure. However, the MAE method was still able to better reconstruct the signal with respect to the other considered methods.

Acknowledgements The authors are thankful to CNPq, CAPES, RENAFAE, FAPERJ and FAPEMIG for the support. This study was financed in part by the Coordenação de Aperfeiçoamento de Pessoal de Nível Superior - Brasil (CAPES) - Finance Code 001. An early version of the paper was presented at XXIII Congresso Brasileiro de Automática (CBA 2020).

Declarations

Conflict of interest The authors declare that they have no conflict of interest.

References

Aad, G., Abbott, B., Abdallah, J., Aben, R., Abolins, M., AbouZeid, O. S., Abramowicz, H., Abreu, H., Abreu, R., Abulaiti, Y., Acharya, B. S., Aad, G., Abbott, B., Abdallah, J., Aben, R., Abolins, M., AbouZeid, O. S., Abramowicz, H., Abreu, H., ... Acharya, B. S. (2017). Topological cell clustering in the ATLAS calorimeters and its performance in LHC Run 1. *European Physical Journal C, 77*, 490. https://doi.org/10.1140/epjc/s10052-017-5004-5

Aaij, R., Akar, S., Albrecht, J., Alexander, M., Albero, A. A., Amerio, S., Anderlini, L., d'Argent, P., Baranov, A., Barter, W., & Benson, S. (2019). Design and performance of the LHCb trigger and full real-time reconstruction in Run 2 of the LHC. *Journal of Instrumentation, 14*(04), P04013. https://doi.org/10.1088/1748-0221/14/04/p04013

Adzic, P., Alemany-Fernandez, R., Almeida, C. B., Almeida, N. M., Anagnostou, G., Anfreville, M. G., Anicin, I., Antunovic, Z., Auffray, E., Baccaro, S., & Baffioni, S. (2006). Reconstruction of the signal amplitude of the CMS electromagnetic calorimeter. *European Physical Journal C, 46s1*, 23–35. https://doi.org/10.1140/epjcd/s2006-02-002-x

Anderson, K., Gupta, A., Merritt, F., Oreglia, M., Pilcher, J., Sanders, H., Shochet, M., Tang, F., Teuscher, R., Wu, H., & Blanchot, G. (2005). Design of the front-end analog electronics for the ATLAS tile calorimeter. *Nuclear Instruments and Methods in Physics Research, 551*(2–3), 469–476. https://doi.org/10.1016/j.nima.2005.06.048

Andrade Filho, L. M., Peralva, B. S., de Seixas, J. M., & Cerqueira, A. S. (2015). Calorimeter response deconvolution for energy estimation in high-luminosity conditions. *IEEE Transactions on Nuclear Science, 39*(5), 3265–3273. https://doi.org/10.1109/TNS.2015.2481714.

Bella, L. A. (2013). Status of the ATLAS liquid argon calorimeter and its performance after two years of LHC operation. *Nuclear Instruments and Methods in Physics Research A, 718*, 60–62. https://doi.org/10.1016/j.nima.2012.11.077

Bertuccio, G., Gatti, E., & Sapietro, M. (1992). Sampling and optimum data processing of detector signals. *Nuclear Instruments and Methods in Physics Research A, 322*, 271–279. https://doi.org/10.1016/0168-9002(92)90040-B

Bondon, P., Benidir, M., & Picinbono, B. (1992). A nonlinear approach to estimate the amplitude of a signal. *IEEE International Conference on Acustic, Speech and Signal Processing, 5*, 301–304. https://doi.org/10.1109/ICASSP.1992.226623

Bos, A. (2007). *Parameter estimation for scientists and engineers* (1st ed.). New York: Wiley. (2007).

Caldwell, A., Gialas, I., Mishra, S., Parsons, J., Ritz, S., Sciulli, F., Sippach, W., Smith, W., Hervas, L., Kötz, U., & Klanner, R. (1992). Design and implementation of a high precision readout system for the zeus calorimeter. *Nuclear Instruments and Methods in Physics Research Section A: Accelerators, Spectrometers, Detectors and Associated Equipment, 321*(1), 356–364. https://doi.org/10.1016/0168-9002(92)90413-X

Cleland, W., & Stern, E. (1994). Signal processing considerations for liquid ionization calorimeters in a high rate environment. *Nuclear Instruments and Methods in Physics Research A, 338*, 467–497. https://doi.org/10.1016/0168-9002(94)91332-3

Collier, M., & Zheng, J. (2014). *Electronic instrumentation and measurement: theory and applications* (1st ed.). CreateSpace Independent Publishing Platform.

Cottingham, W., & Greenwood, D. (1998). *An introduction to the standard model of particle physics*. Cambridge: Cambridge University Press.

Delmastro, M. (2009). Quality factor analysis and optimization of digital filtering signal reconstruction for liquid ionization calorimeters. *Nuclear Instruments and Methods in Physics Research Section A: Accelerators, Spectrometers, Detectors and Associated Equipment, 600*(3), 545–554. https://doi.org/10.1016/j.nima.2008.12.064

Evans, L.R. & Bryant, P. (2008). LHC Machine, *JINST 3*, S08001. 164 p. https://doi.org/10.1088/1748-0221/3/08/S08001.

Fullana, E., et al. (2006). Digital signal reconstruction in the atlas hadronic tile calorimeter. *IEEE Transactions on Nuclear Science, 53*(4), 2139–2143. https://doi.org/10.1109/TNS.2006.877267

Gonçalves, G.I. et al. (2020). Performance of energy estimation algorithms for the tile calorimeter in the ATLAS experiment (in Portuguese), In *Brazilian Conference on Automation* (CBA2020), https://doi.org/10.48011/asba.v2i1.1125.

Gonçalves, G.I. (2021). Simulation code for analysis for the JCAE 2021 Paper. GitHub repository. https://github.com/ingoncalves/jcae-2021-analysis.

Halpern, P. (2010). *Collider: The Search for the World's Smallest Particles*. Wiley.

Haykin, S. (1998). *Neural networks: a comprehensive foundation*. New Jersey: Prentice Hall.

Kay, S. (1993). *Fundamentals of statistical signal processing, estimation theory*. New Jersey: Prentice Hall.

Kleinknecht, K. (1998). *Detector for particle radiation* (2nd ed.). Cambridge: Cambridge University Press.

Knoll, G. F. (2010). *Radiation detection and measurement* (4th ed.). New York: Wiley.

Machikhiliyan, I. (2009). The LHCb electromagnetic calorimeter. *Journal of Physics: Conference Series, 160*, 012047. https://doi.org/10.1088/1742-6596/160/1/012047

Marin, J. L. (2020). Energy reconstruction performance in the ATLAS tile calorimeter operating at high event rate conditions using LHC collision data, In *2020 international conference on systems, signals and image processing (IWSSIP)*. https://doi.org/10.1109/IWSSIP48289.2020.9145451.

Marjanovic, M. (2019). ATLAS tile calorimeter calibration and monitoring systems. *IEEE Transactions on Nuclear Science, 66*(7), 1228–1235. https://doi.org/10.1109/TNS.2019.2921941

Marshall, Z. & Atlas Collaboration (2014). Simulation of Pile-up in the ATLAS experiment. *Journal of Physics: Conference Series, 513,* 022024. https://doi.org/10.1088/1742-6596/513/2/022024.

Muller, H., Budnikov, D., Ippolitov, M., Li, Q., Manko, V., Pimenta, R., Rohrich, D., Sibiryak, I., Skaali, B., & Vinogradov, A. (2006). Front-end electronics for pwo-based phos calorimeter of alice. *Nuclear Instruments and Methods in Physics Research Section A: Accelerators, Spectrometers, Detectors and Associated Equipment, 567*(1), 264–267. https://doi.org/10.1016/j.nima.2006.05.104

Oppenheim, A., & Schafer, R. (2009). *Discrete-time signal processing* (3rd ed.). New Jersey: Pearson.

Peralva, B. S. (2015). The TileCal online energy estimation for the next LHC operation period. *Journal of Physics: Conference Series, 608*, 012043. https://doi.org/10.1088/1742-6596/608/1/012043

Perkins, D. H. (2000). *Introduction to High Energy Physics* (4th ed.). Cambridge: Cambridge University Press.

Pincibono, B., & Duvault, P. (1988). Optimal linear-quadratic systems for detection and estimation. *IEEE Transactions on Information Theory, 34*, 304–311. https://doi.org/10.1109/18.2638

Seixas, J. M. (2015). Quality factor for the hadronic calorimeter in high luminosity conditions. *Journal of Physics: Conference Series, 608*(1), 012044. https://doi.org/10.1088/1742-6596/608/1/012044

Stoica, P., Hongbin, L., & Jian, L. (2000). Amplitude estimation of sinusoidal signals: survey, new results, and an application. *IEEE Transactions on Signal Processing, 48*(2), 338–352. https://doi.org/10.1109/78.823962

The ATLAS and CMS Collaborations. (2015). Combined Measurement of the Higgs Boson Mass in pp Collisions at $\sqrt{s} = 7$ and 8 TeV with the ATLAS and CMS Experiments. *Physical Review Letters, 114*, 191803. https://doi.org/10.1103/PhysRevLett.114.191803

The ATLAS Collaboration. (2014). Monitoring and data quality assessment of the ATLAS liquid argon calorimeter. *Journal of Instrumentation, 9*, P07024. https://doi.org/10.1088/1748-0221/9/07/P07024

Vizireanu, D. N., & Halunga, S. V. (2012). Simple, fast and accurate eight point amplitude estimation method of sinusoidal signals for DSP based instrumentation. *Journal of Instrumentation, 7*,. https://doi.org/10.1088/1748-0221/7/04/P04001

Weng, J. F., & Leung, S. H. (2000). Nonlinear RLS algorithm for amplitude estimation in class a noise. *IEE Proceedings - Communications, 147*(2), 81–86. https://doi.org/10.1049/ip-com:20000182

Wigmans, R. (2017). *Calorimetry: energy measurement in particle physics* (2nd ed.). Oxford: Oxford University Press.

Yin, X., & Cheng, X. (2016). *Propagation channel characterization, parameter estimation, and modeling for wireless communications* (1st ed.). New York: Wiley-IEEE Press.